Astron. Astrophys. 330, 447–452 (1998)

ASTRONOMY AND ASTROPHYSICS

Neural network method for galaxy classification: the luminosity function of E/S0 in clusters⋆

Emilio Molinari[1] **and Riccardo Smareglia**[2]

[1] Osservatorio Astronomico di Brera, Via Bianchi 46, I-23807 Merate (LC), Italy (molinari@merate.mi.astro.it)
[2] Osservatorio Astronomico di Trieste, Via Tiepolo 11, I-34131 Trieste, Italy

Received 24 March 1997 / Accepted 2 October 1997

Abstract. We present a method based on the non-linear behaviour of neural network for the identification of the early-type population in the cores of galaxy clusters. A Kohonen Self Organising Map applied on a three-colour photometric catalogue of objects enabled us to select in each passband the elliptical galaxies. We measured in this way the luminosity function of the E/S0 galaxies selected in this way. Such luminosity functions show peculiarities which disfavour the hypothesis of its universality often claimed for rich clusters and that can be related to the past dynamical history of the cluster as a whole.

Key words: galaxies: clusters: general – galaxies: elliptical and lenticular – galaxies: luminosity function – galaxies: photometry – methods: miscellaneous

Table 1. Cluster parameters

Name	Ref	z	T_{BM}	Obj No.		r lim
				total	gri	
A3594	M96	–	II	456	298	25.0
A3284	M94	0.150	I	453	199	24.5
A3305	M94	0.157	I-II	281	122	22.5
A1689	M96	0.185	I-II	840	585	25.0
A1942	M94	0.226	III	277	167	23.5
MS0418.3-3844	M96	0.339	II	636	323	25.5
Cl2158+0351	M89	0.45	II	291	158	23.5

Notes to the table:
M89: Molinari et al. 1990; M94: Molinari et al. 1994
M96: Molinari et al. 1996
T_{BM}: Bautz-Morgan classification
gri: objects with complete photometry
r lim is the magnitude where the efficiency of the detection algorithm drops to 50%

1. Introduction

By now the determination of the luminosity function (LF) of galaxies in clusters has reached the key point of becoming a true challenge to the supposed universality of its form (as in Colless 1989). Different environment and cluster density conditions are clearly related to different morphological mixtures (Dressler 1980; Whitmore & Gilmore 1993) and therefore the evidence provided by the whole set of LF shapes in the Virgo cluster (Binggeli et al. 1988) claims that one luminosity function for all types of clusters can hardly be supported. The clear presence of two distinct classes of normal and dwarf galaxies and their different dynamical and luminosity evolution can lead to the search of substantial differences from one LF to the other. Unfortunately systematic surveys span a small magnitude range, going from (M^* − 1) to (M^* + 2), and therefore fail to show the different weight that different populations can have (Colless 1989).

Recently Lopez & Yee (1996) showed the LFs of two clusters with different static and dynamic properties which present striking differences. The rich cluster A401 is well fitted by a single Schechter function with a flat faint-end ($\alpha = -1$, in contrast with the value of -1.25 for the universal LF of Colless, 1989) while the fainter galaxies of the poorer cluster A168 follow a steep increase ($\alpha = -1.5$). The different dwarf galaxy mixture should explain the differences, and this naturally relates to the past dynamic history of the cluster.

Also Biviano et al. (1995) found a peculiar feature in the luminosity function of the inner region of the Coma cluster. The two classes of normal and dwarf ellipticals are separated by a 0.5 mag wide gap. The absolute magnitudes of the missing galaxies closely match the change of regime toward dwarf ellipticals measured by Binggeli et al. (1988), which, in the Virgo cluster, remains hidden in the cumulative (E+dE) luminosity function. The need of a composite LF is again called for modelling the behaviour of dynamically evolved clusters.

In this paper we devise a new method for the identification of the early-type galaxy component of clusters, and apply it to

⋆ Based on observations made at the European Southern Observatory (ESO), La Silla, Chile

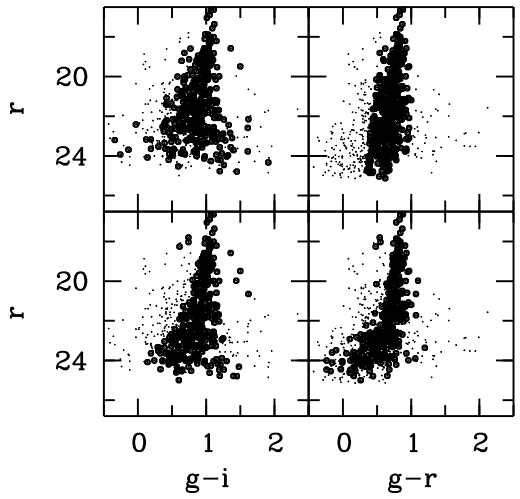

Fig. 1. The classical c-m selection of the early-type sequence in a galaxy cluster works somewhat poorly when more photometric data are available for each object. In the upper two panels we operated a 0.6 magnitude selection around the colours of the c-w sequence determined on the plot. The selection operated in the $g-r$ colour affects in a strange way both the $g-r$ selected faint galaxies and the overall scatter in the $g-i$ plot. The lower panels report the same cluster classified through our ANN procedure for comparison.

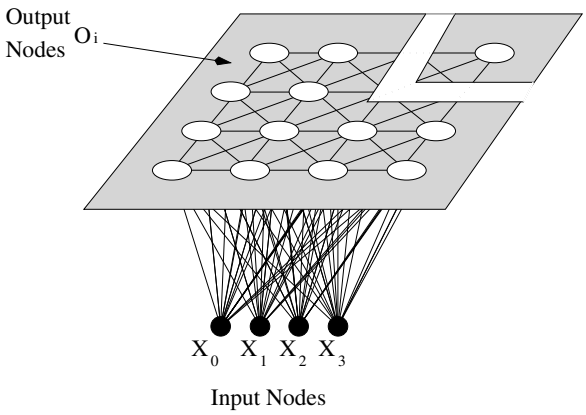

Fig. 2. Example of conventional SOM architecture with continuous-valued input (X_1,.. X_4) and a two dimensional array of output nodes O_i. In our SOM X_j are the normalised photometric values and the output nodes will try to resemble input vectors and to put similar values closer on the map plane. At the end each input vector will be represented by the most similar output node.

a photometric catalogue of 7 rich clusters of galaxies out to a distance of 1–2 core radii.

In Sect. 2 a summary of the observations is presented; Sect. 3 gives an overview of the Self Organising Maps (SOM) which is the artificial neural network (ANN) used for the automatic classification, together with the actual implementation to our data set and the human interpretation of the ANN work. In Sect. 4 we finally study the luminosity function of the ANN-selected early-type galaxies and give support to the hypothesis of a non-universal LF for the cluster cores.

2. The data

Our data-base consists of a collection of photometric catalogues obtained from different observations at the ESO 3.6m telescope (Molinari et al. 1990, 1994, 1996). The seeing during our observations did not fall below 1.6 arcsec, with a median value of the order of 2.0 arcsec. This completely discarded the possibility of performing a visual-based classification of the objects in the fields, in particular the more distant clusters. Nevertheless the whole catalogue gives data for over 6000 objects of 11 clusters, a good fraction of these in three passbands ranging from 5600Å to 9000Å, using the g , r and i Gunn filters. Table 1 lists the subset of 7 clusters analysed in this work, which span a redshift range from near ($z \sim 0.15$) to intermediate ($z \sim 0.5$) when compared with the timescale for dynamic evolution of such structures.

The subset of objects with three colours is the one used to feed the neural network (see next section) in order to attempt a purely photometry-based classification of objects. In the input set this will consist of member and non-member galaxies (interlopers) of different morphological types (and thus different intrinsic colours) and a negligible amount of galactic stars.

Classical approaches to early-type galaxy identification use the robustness of the colour-magnitude relation showed by this kind of galaxies virtually in all clusters (Visvanathan and Sandage 1977, Andreon et al 1997). This relation is quite linear in most cases, but it can be disturbed by photometric errors, especially at the faint end of the luminosity function. In this case a slightly erroneous determination of the background around galaxies which are 4-5 magnitudes fainter than sky brightness might lead to a non-linear c-m sequence for early-type galaxies.

Furthermore, the availability of two colours, as in our case, would lead to two different deviations from linearity and one colour selection can prevent the use of the other data. Molinari (1996) showed the possible implications of the use of rigid, linear boundaries around a c-m sequence determined from the brightest ellipticals. Loosing some faint galaxies in one colour and overestimating the scatter in the other one are the main consequences. Fig. 1 shows the behaviour of such strict boundaries in the upper panels.

We therefore introduce a degree of non-linearity in our detection procedure. Our goal was to avoid loosing all the information left in the data which were obtained with a mean seeing condition. We then used the whole photometric catalogue as a set of vectors in a 4-dimensional space and tried to find a method to arrange these vectors in a sensible way, attempting a classification of the objects. Our efforts aimed to find an objective, automated procedure to single out the concentration represented by the colour-magnitude sequence which is a natural overdensity in our photometric 4-dim space.

The novelty of our approach consists in the use of an unsupervised neural network. Such method works with no input about the *nature* of the data, in contrast with supervised methods

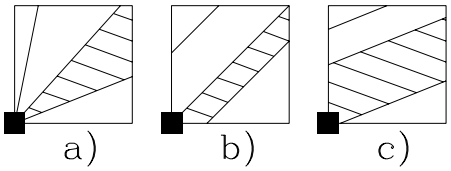

Fig. 3a–c. Slicing the SOM plane: three possibilities for the plane partition are shown. The shaded area represents a particular class; the big square the BECM position (see text). Case **a** and **b** are two-parameter partitions (two angles *or* two coordinates), while **c** needs three parameters (one angle *and* two coordinates). The last one is chosen for the early-type identification.

(see e.g. Naim et al. 1995, Lahav et al., 1995). In the latter case the neural network is first trained with a subset of the data of *known* classification which is fed into the network. Neural network have been proved to be suitable for organising a series of many parameters, mimicking classical human galaxy classification (Lahav et al., 1995) or recognising patterns in pixel-based images (Mähönen & Hakala, 1995).

Our task is somewhat made simpler by the low numbers of parameters, basically the photometric data extracted by means of classical algorithm (see West and Kruszewski, 1981 for a description of INVENTORY).

The whole process of classification is based on the search of structures in the abstract, 4-dimensional space of the magnitude *r*, the two colours *g-r*, *g-i* and the isophotal radius R_{iso}.

3. The classification algorithm

Artificial Neural Netwoks (ANNs) can be roughly divided into two main categories: supervised and unsupervised. The use of one of the two categories depends on how well the data to be classified are known. If a supervised method is used, a well-known and good training set is needed: this implies, however, that any error in classifying the training data set is exported to the general classification. If only a poorly known data set is available for the training procedure, or if detection of clustering in the input data with no a-priori knowledge is desired, an unsupervised method can be used. In our case, we have decided to use a classic unsupervised classification method: the Kohonen Self Organising Maps (SOM).

3.1. The organisation of the 4-dimensional phase space

The SOM algorithm developed by Kohonen (1984) creates a vector function by adjusting weights from N input nodes to M output nodes arranged in a two dimensional grid, i.e. it defines a mapping from the input space R^N (in this case $N = 4$) onto a regular two-dimensional array of nodes. The algorithm is applied to the architecture shown in Fig. 2. There are N normalised continuous-valued inputs, (X_1,.. X_N). The outputs O_i are arranged in a two dimensional array, and are fully connected via the W_{ij} weights to the inputs.

The smallest Euclidean distances $||X - W_i||$, where W_i is the vector with W_{ij} as components, is then usually selected to define the best-matching node:

$$c = \arg\min_i\{||X - W_i||\}$$

Thus X is mapped onto the node c relative to the parameter values W_i. The weights are thus updated for node c and for all nodes in a particular neighbourhood so that the procedure can be iterated for a prefixed number of times.

The final result is a 2-D map which reports the topology of the set of input data in the less distorted way. In the output map similar vectors, that means similar photometric properties for our galaxies, are placed close to each other, while the more the vectors differ, the farther they are placed. If the input set of vectors is suitably chosen, the whole object population will find its (smooth) distribution in the map. Our choice was to extract a random subset of all the objects to be fed into the SOM. The choice was repeated several times but results did not differ in quality of map distribution. We note that each map produced, even with the *same* subset of galaxies, may be different in every run, mostly in the overall orientation. A further manual step is therefore needed to give the same orientation to all the produced maps, so that we can more easily compare them.

3.2. Mapping galaxy types

We used the package SOM_PAK (Kohonen et al. 1995) to create, for each of our clusters, an output 2-D square map with dimensions which are proportional to the number of input data. A direct survey is necessary to understand the relocation on the 2-D map of the classes of interest which compose the input set. In our case it was simple to identify some of the 'true' early-type galaxies selecting a sample of objects that were falling well on the ridge of the colour-magnitude relation in the *r* vs. *g-r* plane. We tried different partitions of the SOM plane and then used as a check the usual colour-magnitude plane, but in the two available colours. After recognising that the brightest elliptical cluster members (BECM) were mapped into one of the corner neurones, we suitably flipped the whole SOM to fix the origin (0,0) as the position of BECM. Fig. 3 shows some possible plane partitions that were explored before choosing the more flexible inclined parallel slicing (panel c in Fig. 3). Although this partition needs three parameters to be defined, it essentially maps the whole object population as a one-dimensional family, namely the coordinate perpendicular to the slicing lines. We are investigating the possibility to fix the location of the BECM point into the SOM map.

The actual selection was then performed on each cluster using the 1-D coordinate which is perpendicular to the slicing. A position histogram was first produced and then the peak which included the (0,0) BECM point was marked as early-type. Fig. 4 shows the location of the E/S0 galaxies in the SOM plane, as well as in the two colour-magnitude planes *r* vs. *g-r* and *r* vs. *g-i*, in which it is easy to recognise the usual *c-m* relation. These are the objects classified as E/S0 in our procedure.

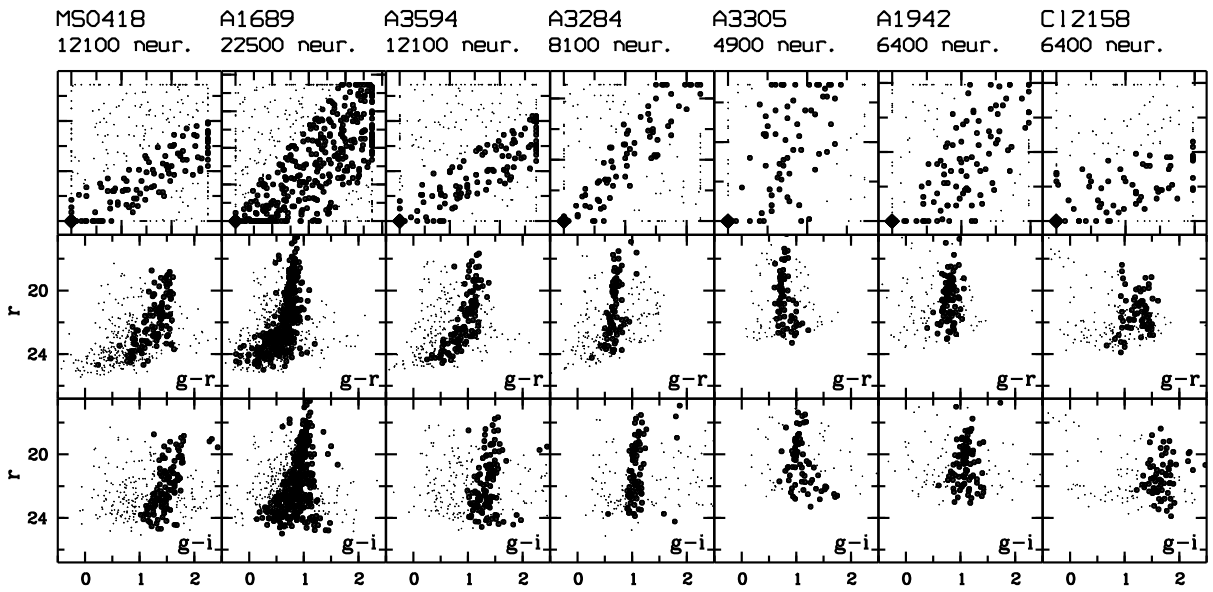

Fig. 4. Identification of the E/S0 galaxies. In the upper panel for each cluster the SOM plane is shown, E/S0 are marked points while small dots show all objects in the catalogue. The filled losange shows the BECM position. In the middle and lower panels the colour-magnitude plots (*r, g-r* and *r, g-i*) shows the early-type galaxies in the mostly used planes.

Table 2. Luminosity function

mag bin	A3284	A3305	A1689	A1942	MS0418.3-3844	Cl2158+0351	A3594	mag bin
-25.25 -24.75	0	0	0	0	0	0	0	16.75 17.25
-24.75 -24.25	0	0	1	0	0	1	1	17.25 17.75
-24.25 -23.75	0	0	0	2	0	1	2	17.75 18.25
-23.75 -23.25	0	1	4	0	0	3	4	18.25 18.75
-23.25 -22.75	1	0	2	1	7	6	3	18.75 19.25
-22.75 -22.25	2	3	6	4	5	3	9	19.25 19.75
-22.25 -21.75	3	5	13	7	6	10	6	19.75 20.25
-21.75 -21.25	2	2	23	9	8	9	7	20.25 20.75
-21.25 -20.75	5	8	25	18	9	13	11	20.75 21.25
-20.75 -20.25	7	7	20	12	13	13	11	21.25 21.75
-20.25 -19.75	9	7	18	6	8	4	5	21.75 22.25
-19.75 -19.25	6	8	18	12	12	4	15	22.25 22.75
-19.25 -18.75	4	6	30	10	17	2	16	22.75 23.25
-18.75 -18.25	5	8	32	7	13	0	10	23.25 23.75
-18.25 -17.75	11	8	26	4	10	0	13	23.75 24.25
-17.75 -17.25	10	7	52	0	7	0	5	24.25 24.75
-17.25 -16.75	5	2	30	0	0	0	0	24.75 25.25
-16.75 -16.25	6	0	45	0	0	0	0	25.25 25.75
-16.25 -15.75	5	0	21	0	0	0	0	25.75 26.25
-15.75 -15.25	1	0	6	0	0	0	–	–
-15.25 -14.75	0	0	0	0	0	0	–	–

Table 3. Summary of gap presence

z range	central M_r	notes
0.15	-17.0	1σ level in the normal to dwarf change of regime
0.15	-21.5	2σ level in the bright zone
0.25	-20.0	2σ level, normal to dwarf change
0.45	-20.0	incompleteness range for one of the cluster begins here
0.45	-22.5	2σ level, bright zone

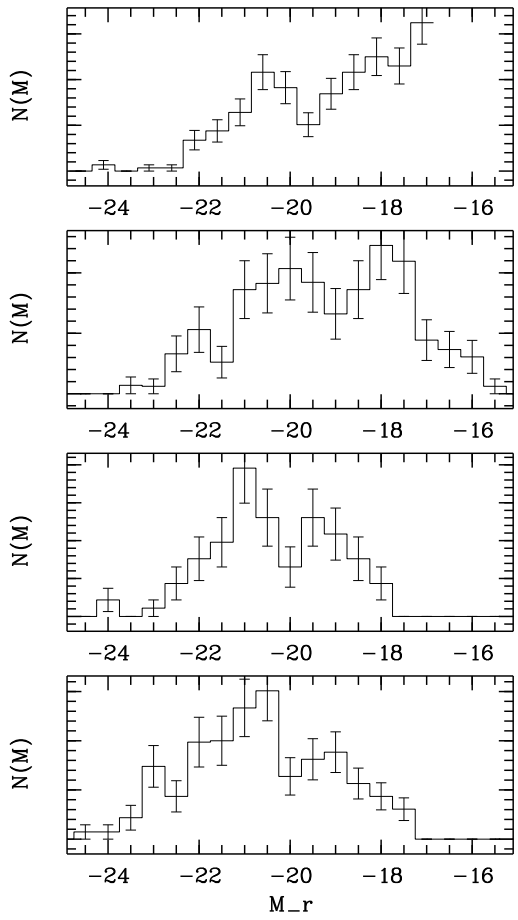

Fig. 5. Luminosity functions for four classes of clusters. In the upper panel we report the LF of the Coma cluster ellipticals by Biviano et al. (1995); in the upper-middle panel our group of *low redshift* ($z \sim 0.15$) clusters; in the lower-middle panel the clusters at *medium redshift* ($z \sim 0.25$); in the lower panel the *high redshift* clusters ($z \sim 0.45$).

We are nevertheless aware that the point (0,0) of the BECM is probably degenerated, in the sense that it may include a whole family of objects where the parameter of the magnitude *g* is the major common factor. We note the possibility that very bright spiral galaxies are included among the BECM, but due to the paucity of such objects identification and subsequent elimination is straightforward. This warning applies to all 7 clusters, but the influence on the LF can be neglected, as it is introducing 1–2 galaxies in the brighter 0.5 mag bin at most. All the ANN selected objects will be then taken as fiducial early-type galaxies in the next section.

The advantage of this selection versus a normal c-m selection is mainly due to the fact that all the parameters are taken simultaneously into account, so that the SOM is able to follow non-linear features which can describe the locus of ellipticals in the phase space. In order to check the method efficiency a set of photometric data was simulated. We included a background modelled as a power-law luminosity distribution similar to what we observe in our fields, and superposed sequence of galaxies with the colours of ellipticals manifesting a c-m relation. We also added a small quadratic coefficient in the c-m relation to mimic our data . The SOM was able to follow the 'curved' c-m ridge down to the position in which the number of superposed ellipticals was close to the number of background objects.

4. The luminosity functions

Since we are confident in the capability of the SOM machine to extract the member E/S0 galaxies from the photometric catalogues, no other corrections for background objects distribution were applied. This is possible because only the member galaxies obey the c-m relation an thus populate the 4-dimensional space in the relative hyper-region. The constraint that our member candidates shall satisfy at the same time the two colour-magnitude relations gives a higher degree of confidence to our assumption.

Table 2 quotes all the frequencies of E/S0 galaxies in 0.5 mag bins. Absolute magnitudes are computed using H_0 = 50 km/s/Mpc and q_0 = 0 Universe. Evolutionary and *k* corrections are computed according to the theoretical models by Buzzoni (1995). The LF of A3594 is quoted in apparent magnitudes at the right-hand side of Table 2; no redshift measure is available so that A3594 will not be included in the rest of this analysis.

The statistic of the numbers in Table 2 is still affected by a somewhat large error, although the magnitude range reaches $M_r = -19.5$ and below, where the dominating population is composed of dwarf galaxies (see Binggeli et al. 1988). We then divided the whole set of clusters in three redshift intervals, centred at $z \sim 0.15$, 0.25 and 0.45 in Fig. 5, where the cumulative luminosity functions are shown. All LFs are computed summing the contribution from each cluster weighted by its total number of E/S0 galaxies. Error bars are computed accordingly. The reason for adding different clusters together is driven by the need to increase the statistic, and can be justified by the similar nature of rich, dynamically evolved clusters. The limiting magnitude for each cluster LF was given in Table 1. The quoted numbers give the significance to the sum of counts extracted from different clusters. In fact the brightest limiting magnitude comes from A3305, which limits the overall cumulative LF reliability to about $M_r \sim -18$. The top panel of Fig. 5 reports the LF for the Coma cluster (a well known virialized cluster, at least in its central region) as determined by Biviano et al. (1995). Where Biviano et al. (1995) find a gap in the region of the change of regime (from normal to dwarfs E) ($M_r \sim -19.5$) we also find significant lack of galaxies in the $z \sim 0.25$ interval. The corresponding regions in the low redshift clusters is less significant, while in the high redshift ones falls just at the beginning of the faint incompleteness limit, showing nevertheless a breakdown at a level higher than 2σ.

Interestingly, significant gaps in the magnitude distribution are present also at brighter magnitudes, next to the bright end of the LF of the low and high redshift clusters. The presence of cD galaxies can lead to depletion in the bright region of the LF, due to cannibalism (Hausman & Ostriker 1978) or to tidal stripping through two-body interactions (Miller 1983). In a hierarchical scenario of cluster virialization the depletion of

the luminosity function could intervene at different magnitudes during the cluster dynamic evolution.

Table 3 summarises the gaps whose presence is suspected. The comments reported in the notes claim further work before a statistically solid basis could be set. We already started a new observational effort to study a sample of nearby ($z < 0.15$) X-ray selected clusters of galaxies which will be deep enough to reach the dwarf galaxies magnitudes and extensive enough to have available thousands of objects with two-colors photometry in each cluster out to about 10 core radii.

5. Conclusions

We have reported a successful trial for isolating a population component in a cluster of galaxies using only a photometric catalogue of objects detected in the direction of the cluster cores. The basis of the analysis is a Kohonen Self Organising Map. This SOM was able to identify a topological structure in the 4-dimensional phase space constituted by the *r* isophotal magnitude, the *g-r* and *g-i* colour indices, together with the isophotal radius R_{iso} of each object.

The only class of objects that could reliably be detected with a single SOM map is the early-type galaxy population, which obeys the colour-magnitude relation. This enabled us to determine the luminosity functions for this class of galaxies in the core of rich, dynamically evolved clusters, out to 1-2 R_{core}. The LFs thus measured show peculiarities such as magnitude bins with particularly low number of objects, especially in the intermediate region between the E/S0 and the dwarf E galaxies. This irregularity or bimodality seems to be common to highly evolved, rich clusters, but still awaits further confirmation and a definite explanation.

References

Andreon, S., Davoust, E., Heim, T., 1997, A&A 323, 337
Binggeli, B., Sandage, A., Tamman, G.A., 1988, ARA&A 26, 509
Biviano, A., Durret, F., Gerbal, D., Le Fevre, O., Lobo, C., Mazure, A., Slezak, E., 1995, A&A 297, 610
Buzzoni, A. 1995, ApJS 98, 69
Colless, M., 1989, MNRAS 237, 799
Dressler, A., 1980, ApJ 236, 351
Hausmannn, M.A., Ostriker, J.P., 1978, ApJ 224, 320
Kohonen, T., 1984, Self-Organization and Associative Memory Springer-Verlag, Berlin
Kohonen, T., Hynninen, j., Kangas, J, Laaksonen, J., 1995, SOM_PAK: The Self-Organiser Map Program Package Version 3.1
Lahav, O., Naim, A., Buta, R.J., Corwin, H.G., de Vacouleurs, G., Dressler, A., Huchra, J.P., van den Bergh, S., Raychaudhury, S., Sodré Jr., L., Storrie-Lombardi, M.C., 1995, Science 267, 859
Lopez, O., Yee, H.K.C., 1996, in: proceedings of "Fresh Views of Elliptical Galaxies", Eds. A.Buzzoni, A.Renzini, A.Serrano (ASP: San Francisco) p.279
Mähönen, P.H.,, Hakala, P.J., 1995, ApJ 452, L77
Miller, G.E., 1983, ApJ 268, 495
Molinari, E., 1996, in: proceedings of "Fresh Views of Elliptical Galaxies", Eds. A.Buzzoni, A.Renzini, A.Serrano (ASP: San Francisco) p.275
Molinari, E., Buzzoni, A., Chincarini, G., 1990, MNRAS 246, 576
Molinari, E., Banzi, M., Buzzoni, A., Chincarini, G., Pedrana, M.D., 1994, A&AS 103, 245
Molinari, E., Buzzoni, A., Chincarini, G., 1996, A&AS 119, 391
Naim, A., Lahav, O., Sodre, L. Jr., Storrie-Lombardi, M.C., 1995, MNRAS 275, 567
Visvanathan, N., Sandage, A., 1977, ApJ 216, 214
West, R.M., Kruszewski, A., 1981, Ir. Astr. J. 15, 25
Whitmore, B.C., Gilmore, D.M., 1991, ApJ 367, 64

This article was processed by the author using Springer-Verlag LaTeX A&A style file *L-AA* version 3.